Effects of filling in $CoSb_3$: Local structure, band gap, and phonons from first principles

Daehyun Wee
Research and Technology Center, Robert Bosch LLC, Palo Alto, California 94304, USA

Boris Kozinsky
Research and Technology Center, Robert Bosch LLC, Cambridge, Massachusetts 02142, USA

Nicola Marzari
Department of Materials Science and Engineering, Massachusetts Institute of Technology, Cambridge, Massachusetts 02139, USA

Marco Fornari
Department of Physics, Central Michigan University, Mt. Pleasant, Michigan 48859, USA

(Received 26 September 2009; revised manuscript received 22 December 2009; published 21 January 2010)

We use *ab initio* computations to investigate the effect of filler ions on the properties of $CoSb_3$ skutterudites. We analyze global and local structural effects of filling, using the Ba-filled system as an example. We show that the deformation of Sb network induced by the filler affects primarily nearest neighboring Sb sites around the filler site as the soft Sb rings accommodate the distortion. Rearrangement of Sb atoms affects the electronic band structure and we clarify the effect of this local strain on the band gap. We compute the phonon dispersions and identify the filler-dominated modes from the lowest-frequency optical modes at Γ. Their weak dispersion across the Brillouin zone indicates that they are localized and a force-constant analysis shows that the filler vibration is strongly coupled with nearby Sb atoms.

DOI: 10.1103/PhysRevB.81.045204 PACS number(s): 84.60.Rb, 31.15.es, 63.20.dk

I. INTRODUCTION

Thermoelectricity provides a fully solid-state solution for power generation and is considered as an attractive option for combined heat and power systems or compact waste heat recovery systems. Current application of thermoelectric materials in power generation, however, only covers a niche area because of their low efficiency and limited reliability. Though the performance of the conventional thermoelectric materials based on Bi_2Te_3 can be improved by various approaches including nanostructuring,[1] its application in power generation remains a challenging task due to its relatively low operating temperature. During the last decade or so, new thermoelectric materials have been pursued for higher performance and extended temperature regimes. Among these materials, skutterudites based on $CoSb_3$ extend the operating temperature up to around 900 K, which makes them promising materials for power generation applications.

The skutterudite structure can be described as a corner sharing network of heavily tilted pnictogen octahedra with a transition metal, which is typically Co or Fe, in the center (Fig. 1). The space group is *Im*3 (n. 204) with four formula units in the primitive cell: the transition metal is in the 8*c* Wyckoff position and the pnictogen in 24*g*. The pnictogen network forms cages around the *a* position in which a guest atom, or filler, can be placed. In general, electronegativity differences among constituents of the octahedral host structure are relatively small and bonding is mostly covalent. The structure is known to be chemically stable, with substantial degrees of freedom in doping and alloying on all sites to obtain an optimized composition for specific purposes. Skutterudites typically maintain large carrier mobilities. Morelli *et al.*[3] showed that the mobility of *p*-type $CoSb_3$ samples doped in the range of 2.6×10^{17}–4.1×10^{18} cm^{-3} were in the range between 1800 and 2800 $cm^2\ V^{-1}\ s^{-1}$. In addition, even with moderately high carrier density, skutterudites show Seebeck coefficients in the order of a few hundred microvolts per Kelvin.[3,4]

In the classical picture, heavy filler atoms in skutterudite crystals undergo isolated vibrations, commonly referred to as rattling, that lower the thermal conductivity by scattering off phonons in a random way.[5] This is the commonly cited reason for the low thermal conductivity in the class of materials. However, this picture has been challenged in recent investigations. Koza *et al.*[6] found evidence of phase coherence in filler vibrations from neutron-scattering experiments of $(La,Ce)Fe_4Sb_{12}$.

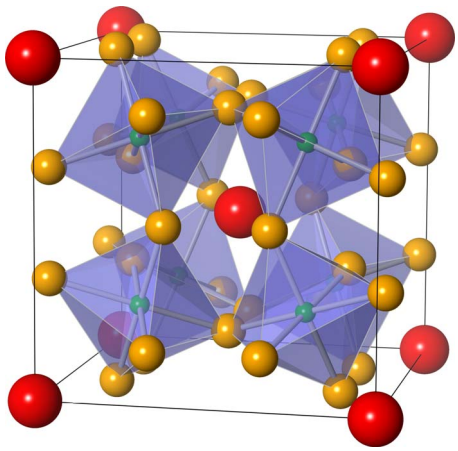

FIG. 1. (Color online) Crystal structure of filled skutterudites. Transition metals, pnictogens, and fillers are presented as small, medium-sized, and large spheres, respectively. Visualized with VESTA (Ref. 2).

The filler's effectiveness as a scattering center of heat-carrying phonons depends on the amount of anharmonicity in its motion and coupling to other components of the crystal. In earlier works, the bare filler vibration frequency, which is the frequency of the vibration of a filler when every other atom is frozen, showed a significantly different value from the actual frequency of the filler-dominated mode observed in phonon dispersion.[7,8] These results imply that there exists a strong interaction between the motion of the filler and those of nearby atoms. The potential experienced by the filler remains parabolic under a substantially large displacement of the filler,[7,9] disputing the anharmonicity of the isolated motion. Thus, the exact nature of the effect of fillers still remains not clearly understood.

There exist number of theoretical and experimental studies on skutterudites and we refer to Refs. 5, 10, and 11 for exhaustive reviews on these materials and related theoretical approaches. Most of previous computational studies were focused either on unfilled $CoSb_3$ (Refs. 12–14) or on experimentally synthesized compounds of filled skutterudites.[8,15,16] In this paper, a slightly different venue is explored. We treat filling as a perturbation added to the unfilled $CoSb_3$ and attempt to develop additional insight by constructing supercells with varying degrees of filling and by imitating several aspects of the effects of fillers independently. In order to separate the effects of different transition metals (e.g., Fe) from the effects of filling, the composition of the host structure is fixed to be $CoSb_3$, despite the difficulty of synthesizing $CoSb_3$ systems filled to a significant fraction.[17] This simplification enables us to separately investigate various effects of filling—structural distortions around fillers, effects of electron transfer from the filler, and filler-induced vibrational characters. A study in a similar spirit, dealing with the effects of defects and impurities, was reported in Refs. 18 and 19.

The paper is organized as follows. In Sec. II, we briefly summarize computational methodology and structures investigated. Results are presented in Sec. III. Global and local structural considerations are presented first. We then continue with a discussion of the electronic properties and conclude with a discussion of the phonon dispersions.

II. METHODOLOGY

Calculations are performed using density-functional theory[20,21] and density-functional perturbation theory (DFPT) (Ref. 22) with QUANTUM-ESPRESSO,[23] using an local-density approximation (LDA) functional.[24] Transport properties, such as electronic conductivity and the Seebeck coefficient, are studied by solving the Boltzmann transport equation under constant relaxation-time approximation, with the BOLTZTRAP package.[25] Thermodynamic properties, including thermal expansion, are estimated within the statically constrained quasiharmonic approximation,[26] using the VLAB thermodynamics package.[27]

Our primary focus is given to Ba-filled $CoSb_3$ systems while Na, K, Ca, and Sr-filled systems are also studied in order to investigate trends across a wider chemical space. $CoSb_3$ skutterudites, both unfilled and fully filled with Na, K, Ca, Sr, and Ba, are considered using a body-centered-cubic unit cell with 16(+1) atoms. The compounds with uniform 50% filling are modeled with a simple-cubic (SC) unit cell of 32+1 atoms. We represent 25% and 75% Ba-filled structures with tetragonal (TetP) $1\times1\times2$ supercell. One more ordering of 50% filling is also considered with a similar tetragonal supercell (TetP). Finally, a $2\times2\times2$ simple-cubic cell with the filling fraction of 6.25% (1/16) is used to investigate the structure of the filler-induced distortion. Atomic cores are described by separable[28] norm-conserving pseudopotentials[29] (Na, K, and Sb) and ultrasoft pseudopotentials[30] (Ca, Co, Sr, and Ba), which are all available in public.[23,30] Spin-orbit coupling is not included in our calculations since the effect of spin-orbit interactions is known to have relatively minor effects in skutterudites.[12]

A kinetic-energy cutoff of 30 Ry is used for all our electronic structure calculations. A $6\times6\times6$ **k**-point grid is employed for body-centered-cubic cells and equivalent sampling is used for larger cells. For phonon calculations, the dynamical matrix is explicitly computed on a $2\times2\times2$ **q**-point grid by linear-response DFPT calculations, whose result is later Fourier interpolated onto a finer mesh.

III. RESULTS

A. Global and local structural changes under filling

In order to investigate the effect of filling on the global crystal structure of skutterudites, we calculate the equilibrium lattice parameter a_0 as a function of the filling ratio for several filler species. Full variable cell relaxation has been performed using the Broyden-Fletcher-Goldfarb-Shanno method[31] until the force on each atom becomes smaller than 10^{-4} Ry/bohr and the stress over the structure is less than 0.5 kbar. The results are presented in Fig. 2. We note that the lattice parameter increases linearly with the filling ratio, in good agreement with Vegard's law. Also, for a given filling fraction, the amount of lattice parameter increase is correlated with the size of the filler ion, as determined using Shannon radii.[33] It is worth noting that the trend is not monotonic for all filler atoms but it is linear within each chemical group. This can be rationalized by taking into account that the amount of charge transferred to the lattice from higher-valence fillers is larger than from lower-valence fillers of similar size. Unfilled $CoSb_3$ lattice parameter in ground state is calculated at 8.972 Å, which is somewhat smaller than the experimental value 9.035(1) Å at room temperature,[32] as expected from LDA calculations. When we include the zero-point motion within the quasiharmonic approximation, the equilibrium lattice parameter is increased to 9.00(0) Å. When we add the effect of thermal expansion and minimize the free energy, the lattice parameter becomes 9.01(7) Å at 300 K, which is closer to the experimental value. The locations of Sb atoms in unfilled $CoSb_3$ are fixed by two internal coordinate symmetry parameters y and z within the space group $Im3$ (n. 204). As shown in Table I along with parameters for other compounds, our values of these parameters are close to experimental values.[34]

We study the internal distortion introduced by the filler and its range of influence by analyzing the relaxed atomic structure in a large supercell (SC $2\times2\times2$) containing 256

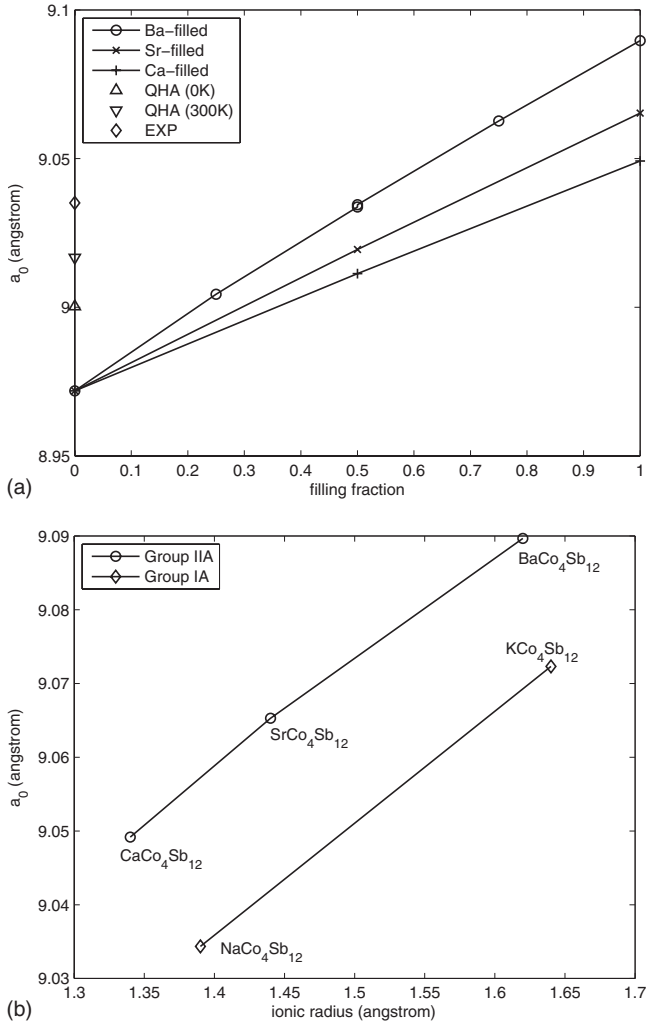

FIG. 2. (a) Lattice parameter a_0 versus filling fraction. QHA: calculated values from statically constrained quasiharmonic approximation and EXP: experimental value (Ref. 32). (b) Lattice parameter a_0 versus the ionic radius of the filler atom.

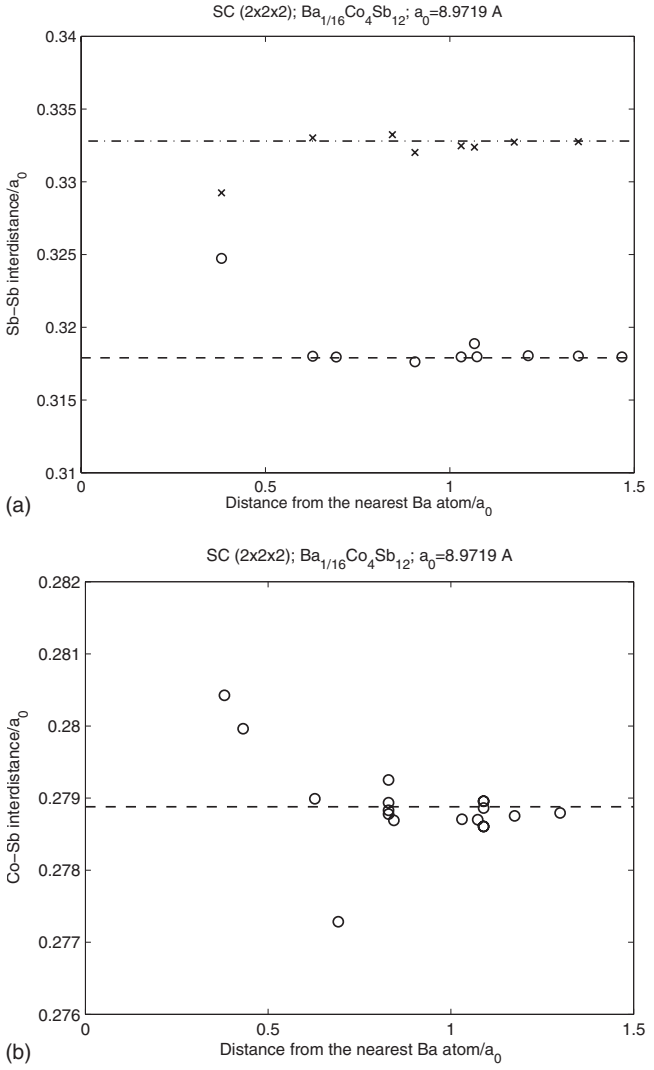

FIG. 3. (a) Length of closest Sb-Sb pairs versus the distance of the pair from its nearest Ba filler atom (in units of a_0). Circles: transverse pairs; crosses: longitudinal pairs; and reference lines represent lengths in unfilled $CoSb_3$. (b) Length of closest Co-Sb pairs as a function of the distance from the filler site.

+1 atoms or Ba filling fraction of 1/16. Closest Sb-Sb pairs can be classified into two distinct groups: each Sb atom belongs to an orthogonal ring consisting of four Sb atoms, with two opposite edges facing a filler site. The alignment of each pair can be either longitudinal along the direction connecting two nearest filler sites or transverse to the direction. In unfilled $CoSb_3$, longitudinal pairs are longer than transverse ones. Filling, however, introduces local stress and rearranges Sb atoms, making transverse pairs longer and longitudinal pairs shorter. This effect is shown in Fig. 3, where the lengths of pairs just beside a Ba atom are significantly different from those observed in unfilled $CoSb_3$. However, the effect is localized around filler sites. The next-nearest pairs barely see the presence of the filler and the length of Sb-Sb pairs rapidly approaches the corresponding value in the unfilled $CoSb_3$, as a function of the distance from the filled site. On the other hand, Co-Sb distances are apparently less responsive and do not show as much variation due to the insertion of Ba atoms. These observations reveal that the over-

TABLE I. Lattice and symmetry independent parameters. Values for unfilled $CoSb_3$ are compared to experimental data (Refs. 32 and 34).

	$BaCo_4Sb_{12}$	$SrCo_4Sb_{12}$	$CaCo_4Sb_{12}$	$CoSb_3$	$CoSb_3$ (Refs. 32 and 34)
a_0(Å)	9.090	9.065	9.049	8.972	9.035(1)
y	0.3391	0.3366	0.3345	0.3335	0.33537
z	0.1629	0.1617	0.1607	0.1589	0.15788

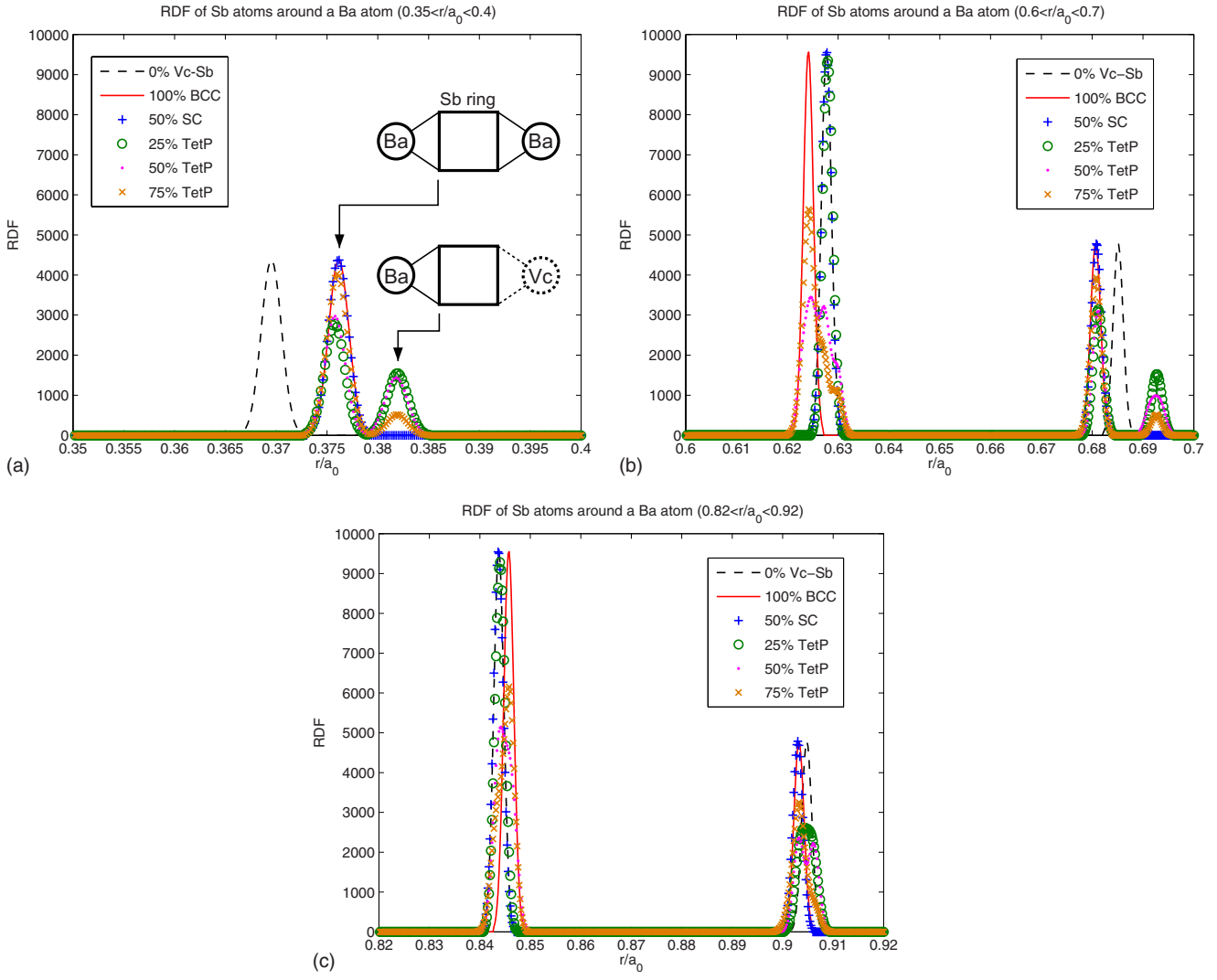

FIG. 4. (Color online) Radial distribution function of Sb atoms around a Ba atom at various filling fractions, shown in an arbitrary unit. The distance of each Sb atom from a Ba atom is normalized by the lattice parameter a_0. For the unfilled case (dashed), the radial distribution of Sb atoms around a vacant filler site is presented instead. (a) $0.35<r/a_0<0.4$, (b) $0.6<r/a_0<0.7$, and (c) $0.82<r/a_0<0.92$.

all structural effect of filling is rather localized around each filler site due to softness of Sb rings.

The locality of the internal distortion introduced by the filler can be also recognized in Fig. 4, where the radial distribution function of Sb atoms around a Ba atom is presented at various filling fractions. Distances are normalized by a_0, which varies with the filling fraction (Fig. 2). For filled compounds, the nearest-neighboring group of Sb atoms around a Ba atom, shown in Fig. 4(a), exhibits two peaks: one around $0.375a_0$ and the other around $0.38a_0$. This splitting is due to local structural characters. As mentioned earlier, every Sb atom is sitting on a Sb ring between two nearby filler sites. At least one nearby filler site of the ring on which the nearest-neighboring group sites is occupied by a Ba atom. The other filler site can be either filled or left vacant. If both filler sites are filled, the Sb ring is squeezed from both sides, resulting in the peak at $0.375a_0$. Alternatively, the Sb ring is only pushed away by the Ba atom on one side without any repulsion from the other side and this corresponds to the peak at $0.38a_0$. The same mechanism contributes to the split between $0.68a_0$ and $0.69a_0$ in Fig. 4(b) of the third-nearest-neighboring group, which shares the same Sb rings with the nearest-neighboring group.

On the other hand, the second-nearest-neighboring group of Sb to the filling site (that does not share the same Sb rings with the nearest-neighboring group) shows a relatively small splitting of the peak at $0.63a_0$. This small splitting is sensitive to the filling of the other nearby filler sites. As the distance from a Ba filler atom site further increases, the radial distribution function quickly approaches that of unfilled $CoSb_3$ and there exists no clear splitting observed beyond the third-nearest Sb group, as shown in Fig. 4(c). In summary, the filler structurally affects the Sb rings nearby but the change is limited only up to the nearest-neighboring Sb rings.

B. Effect on the electronic structure

Unfilled $CoSb_3$ is a direct-gap insulator with a moderate band gap, which is very sensitive to structural parameters. As

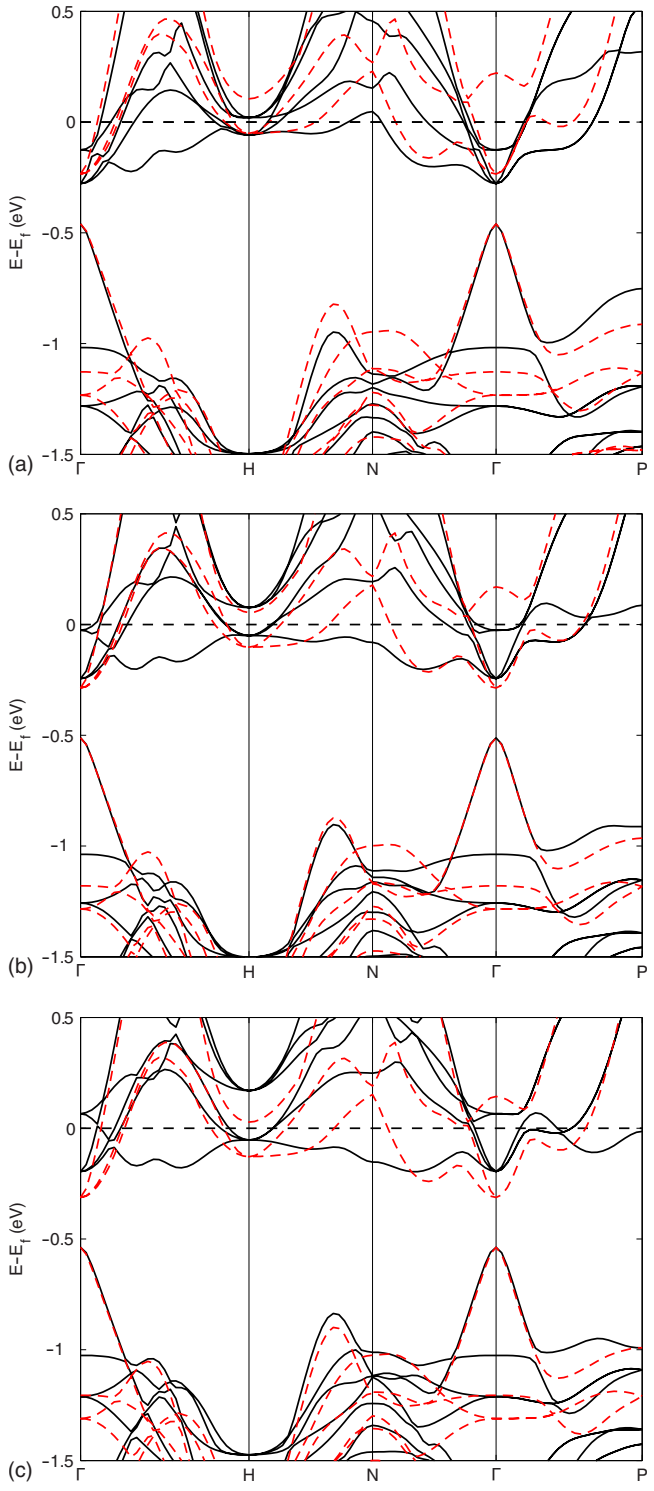

FIG. 5. (Color online) Band structures of (a) $BaCo_4Sb_{12}$, (b) $SrCo_4Sb_{12}$, and (c) $CaCo_4Sb_{12}$, presented with solid lines. The energy reference is set to the Fermi level. For comparison, the band structure of $CoSb_3$ is also plotted with dashed lines, aligned in a way that it shares the same top of the valence band at Γ.

the result, experimental measurements of the band gap are relatively scarce and show significant variations depending on the methodology. Rakoto *et al.*[35,36] performed Shubnikov-de Haas studies and reported 35 ± 2 meV. Mandrus *et al.*[37] deduced 50 meV from resistivity measurements. In the present work, the band gap, E_g, is 0.225 eV for unfilled $CoSb_3$, which is comparable to previously reported values in other calculations.[8,13,14,38]

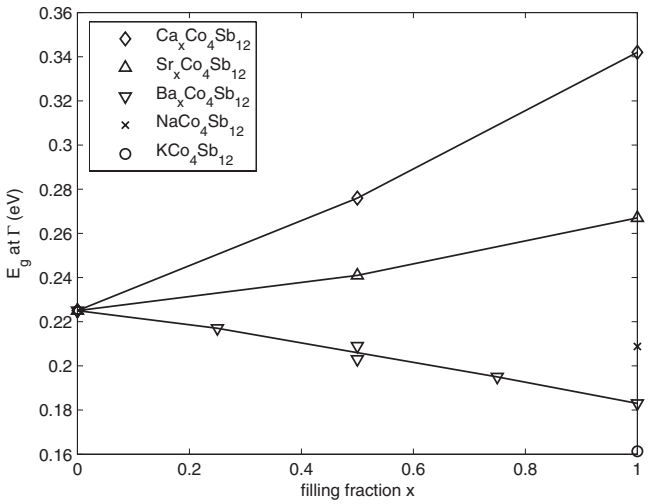

FIG. 6. LDA band gap (eV) at Γ as a function of filling fraction and filler element. Na and K-filled compounds are only showed in fully filled configurations.

While the bottom of the conduction bands around the gap is relatively flat, the top of the highest valence band exhibits a strongly dispersive character near Γ. Figure 5 illustrates the computed band structures of $BaCo_4Sb_{12}$, $SrCo_4Sb_{12}$, and $CaCo_4Sb_{12}$. By projecting the states onto atomic orbitals, we see that the bottom of the conduction manifold is dominated by a filler-derived *s* band everywhere in the Brillouin zone except near Γ, where it retains the character of Co *d* and Sb *s*. The top of the valence band at Γ derives from an antibonding combination of Sb *p* states around Sb rings[13,39] or alternatively it may be seen as a bonding combination between a Co atom and Sb atoms around it.[14] Unfilled $CoSb_3$ is an intrinsic semiconductor while any significant amount of filling turns it into a formally metallic system due to charge transfer from the electropositive filler atom to the crystal matrix. In these metallic configurations, the gap above the dispersive antibonding state of Sb *p* states at Γ is still identifiable, which we shall refer as the band gap for those configurations. The band gaps of all the configurations are summarized in Fig. 6.

TABLE II. LDA band gap (eV) at Γ for structures under pressure.

	a_0 (Å)	P (kbar)	E_g (eV)
$BaCo_4Sb_{12}$	8.999	31.7	0.263
	9.090	≈0	0.183
	9.181	−27.1	0.108
$CoSb_3$	8.882	33.6	0.318
	8.972	≈0	0.225
	9.062	−28.3	0.134

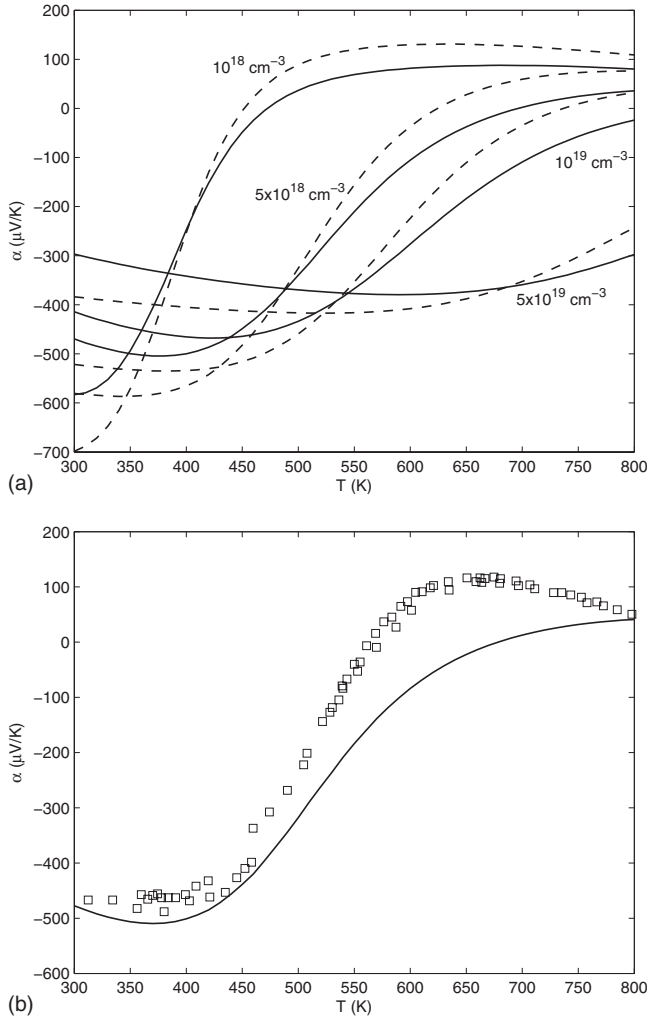

FIG. 7. (a) The Seebeck coefficient (μV/K) computed from the band structure of unfilled $CoSb_3$ (solid) and that of $CaCo_4Sb_{12}$ (dashed) for *n*-type samples. The labels indicate the ionized donor concentration assumed for the band structure of unfilled $CoSb_3$. For $CaCo_4Sb_{12}$, charge is compensated to maintain its $CoSb_3$ host structure isoelectronic to that of the corresponding unfilled $CoSb_3$ band structure. (b) Comparison to an experimental measurement. Solid: computed from the band structure of unfilled $CoSb_3$, assuming an ionized donor concentration of 4.54×10^{18} cm^{-3} and squares: experimental data in Ref. 4 (1CS10).

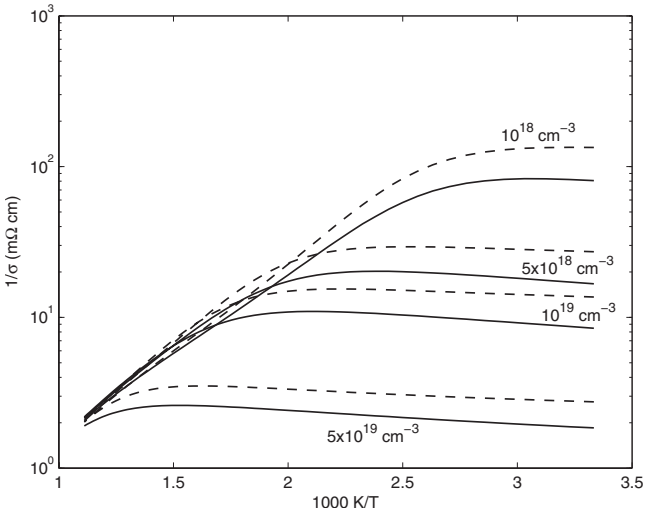

FIG. 8. The resistivity computed from the band structure of unfilled $CoSb_3$ (solid) and that of $CaCo_4Sb_{12}$ (dashed) for *n*-type samples, assuming $\tau=2.5\times10^{-14}$ s. The same rule for defining the ionized donor concentration is employed as that in Fig. 7.

At the zone center, both the top of the highest valence band and the bottom of the lowest conduction band are derived from covalent bonding/antibonding states. These energy levels are sensitive to the distances between participating atoms and can thus be affected by the local distortion introduced by the filling. This, in turn, results in a change in the band gap at Γ. The following trend is recognized in our calculations: with an increased covalent overlap induced by pressure, a compressed structure with a smaller lattice parameter exhibits a band gap larger than that of the equilibrium or expanded structures. The trend is shared by the unfilled structure and the Ba-filled one, hinting that this is independent from a specific chemistry of a filler (Table II). We note that a similar effect can also be introduced by different ionic radii of fillers, thus changing the lattice parameter: $CaCo_4Sb_{12}$ shows a smaller lattice parameter than that of $BaCo_4Sb_{12}$ (Fig. 2) and accordingly exhibits a larger band gap than that of $BaCo_4Sb_{12}$ (Fig. 6).

An additional effect of filling is the charge transfer from the electropositive filler to the $CoSb_3$ host structure. To separately address this direct effect from the indirect distortion-induced changes, the band structure of $BaCo_4Sb_{12}$, whose atomic locations are fixed at those of unfilled $CoSb_3$, is computed (denoted as "unrelaxed $BaCo_4Sb_{12}$," after on). The band gap at Γ turns out to be 0.6 eV, which is significantly larger than the corresponding value of the fully relaxed $BaCo_4Sb_{12}$ or that of unfilled $CoSb_3$, indicating that introduction of extra electrons into the host structure of $CoSb_3$ increases the band gap. Also, by adding extra electrons compensated by a jellium in the computation of the same unfilled $CoSb_3$ structure we notice that the band gap at Γ increases. The trend is also confirmed by the fact that the band gaps in alkali-metal-filled compounds are predicted to be lower than those containing alkaline-earth fillers of similar ionic size, due to smaller transfer of charge, as shown in Fig. 6.

Starting from the band structure, we can estimate electronic transport properties using a semiclassical Boltzmann transport approach with the constant relaxation-time approximation.[25] Fig. 7 shows the Seebeck coefficient computed for doped *n*-type samples by using the band structure of unfilled $CoSb_3$ and that of $CaCo_4Sb_{12}$. The qualitative behaviors of the computed Seebeck coefficients closely resemble those observed in experiments,[4] as shown in Fig. 7(b). Agreement with experiment is good at low-temperature regime (around 300 K). Our result qualitatively captures the transition from *n* type to *p* type with increasing temperature, which is experimentally observed, though the values of the Seebeck coefficient and the transition temperature deviate from experimental observations in the high-temperature regime. This is not surprising since the contribution from mul-

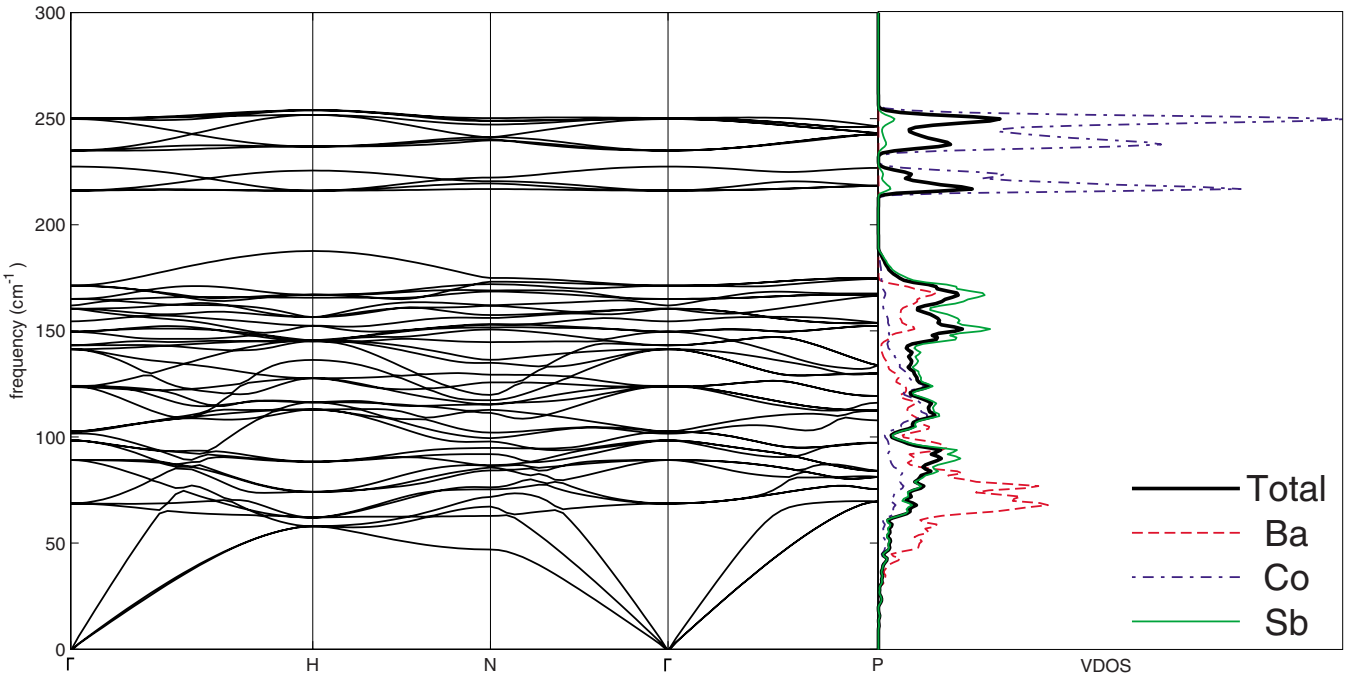

FIG. 9. (Color online) Phonon dispersion curves and computed vibrational density of states of $BaCo_4Sb_{12}$ with contribution from each element, normalized by the number of atoms of the participating elements in the unit cell.

tiple bands invalidates the constant relaxation-time approximation. In addition, the concentration of ionized donors can vary with temperature while we assume it is constant (4.54×10^{18} cm^{-3}) here. The band structure of $CaCo_4Sb_{12}$ exhibits a relatively flat bottom of the conduction band, which results in noticeable improvement of the Seebeck coefficient at low temperature. This advantage is, however, not sustained at high temperature, where the Fermi distribution widens and contributions from multiple bands become important. Electrical resistivity computed with a constant relaxation time of 2.5×10^{-14} s is also shown in Fig. 8. We note that, unlike the Seebeck coefficient, the electrical resistivity is inversely proportional to the actual value of the relaxation time even under the constant relaxation-time approximation, making the applicability of the approximation more dubious than that for the Seebeck coefficient.

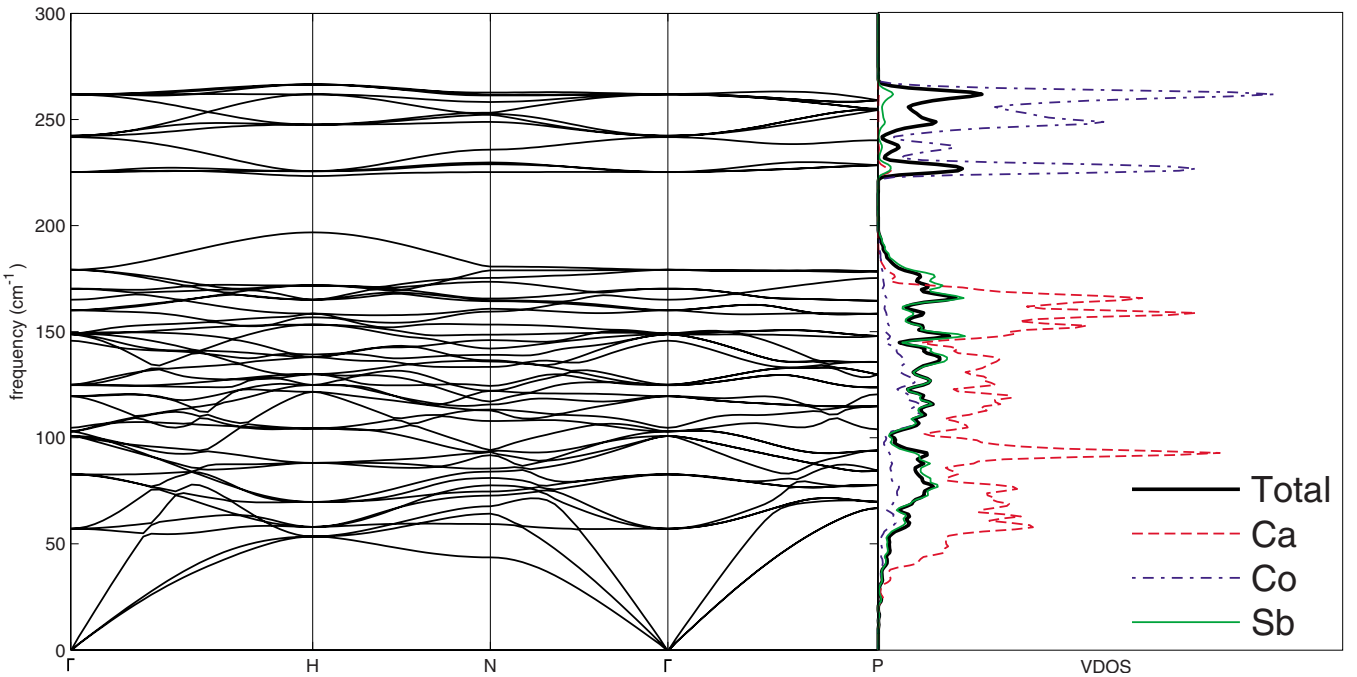

FIG. 10. (Color online) Phonon dispersion curves and computed vibrational density of states of $CaCo_4Sb_{12}$ with contribution from each element, normalized by the number of atoms of the participating elements in the unit cell.

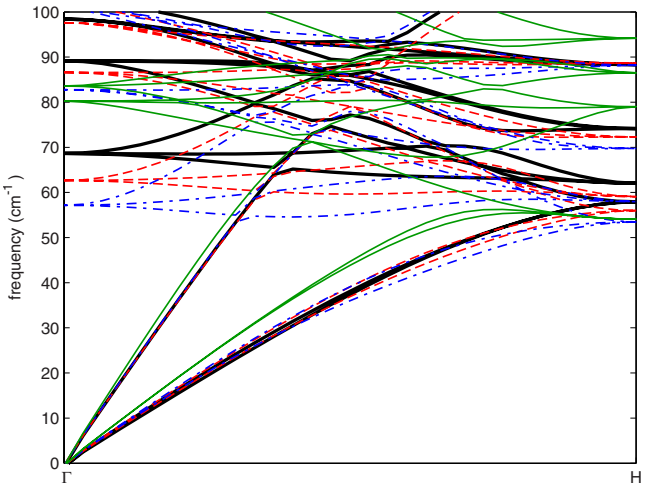

FIG. 11. (Color online) Phonon dispersion curves of $BaCo_4Sb_{12}$ (thick solid), $SrCo_4Sb_{12}$ (dashed), $CaCo_4Sb_{12}$ (dash dot), and $CoSb_3$ (thin solid) along Δ in the low-frequency regime.

C. Vibration spectra

In order to understand the effect of the filler on the thermal transport in skutterudites, we start by calculating the vibration spectrum using density-functional perturbation theory, which allows us to analyze the full phonon-dispersion information in the Brillouin zone. This methodology was successfully used in computing phonon dispersions of $CoSb_3$ and $TlFeCo_3Sb_{12}$ in a previous study.[8] In Figs. 9 and 10, we present the phonon-dispersion curves for $BaCo_4Sb_{12}$ and $CaCo_4Sb_{12}$. Phonon density of states with contribution from each element is also shown. $SrCo_4Sb_{12}$ exhibits similar vibrational structure somewhere between those of $BaCo_4Sb_{12}$ and of $CaCo_4Sb_{12}$. In Fig. 11, we compare the low-frequency vibrational spectra in various compounds along the Δ line in the Brillouin zone. All of our calculated spectra exhibit relatively large gaps at about 200 cm^{-1}. In $BaCo_4Sb_{12}$ the Co-dominated manifold above 200 cm^{-1} shows a clear splitting into two groups, which was also observed in $CoSb_3$.[40] The splitting disappears in $CaCo_4Sb_{12}$. In contrast to the calculations in Ref. 8, no gap is clearly identified at about 100 cm^{-1} but we also find a rather low density of states there.

Except in $CaCo_4Sb_{12}$, where Ca participates in higher optical modes as well due to its smaller mass, strong contributions from fillers are found in the range between 50 and 100 cm^{-1} for both Ba and Sr fillings. Accordingly, we identify the filler-dominated modes as relatively flat manifolds in that frequency range, forming the lowest optical modes (F_u) at Γ. The frequencies of these modes at the zone center are listed in Table III. The weak dispersion of these bands points to the localized nature of these vibrations. This could suggest the fillers' role as mostly decoupled random scattering centers for acoustic phonons that carry thermal current. Above these lowest optical modes lie the second lowest optical modes (F_g) at Γ that predominantly have Sb character, also reported in Table III. The great similarity of these optical modes of filled compounds to the lowest optical modes observed in unfilled $CoSb_3$ has not drawn much attention. Unfilled $CoSb_3$ shows the lowest optical mode (F_u) at 80 cm^{-1} and the second lowest one (F_g) at 83 cm^{-1}. These modes are all Sb dominated and exhibit little dispersion, indicating that they are also localized. The characteristic motion of Sb rings in each of these modes can be characterized either as translation for F_u modes or as in-plane ring rotation for F_g modes. In filled compounds the lowest optical modes (F_u) are dominated by the motion of the fillers but the associated motion of Sb rings in these optical modes can still be characterized as translation (Fig. 12). The next lowest optical modes in filled compounds are more or less identical to the rotationlike F_g modes in unfilled $CoSb_3$ (Fig. 13). Based on the similarity between the lowest optical modes of filled and unfilled compounds, it is natural to consider the filler-dominated lowest optical modes in filled compounds as originating from the lowest optical modes of unfilled $CoSb_3$, rather than as something solely created by fillers. Sb ring vibrations are not substantially mixed with the vibrations of the other Sb rings in unfilled $CoSb_3$, exhibiting only a small difference between the frequencies of F_u and F_g modes. The introduction of a filler makes the vibrations of the nearby Sb rings weakly coupled, resulting in a greater splitting between the F_u and F_g modes in filled compounds. Strong hybridization between filler motions and Sb motions is, hence, expected.

The bare frequency of the filler vibration was calculated earlier to be about 90 cm^{-1} for Ba and Sr, assuming only the filler motion in its harmonic potential.[9] Via our analysis of the force constants obtained from the linear-response calculations, we obtain the bare frequencies of 101 cm^{-1} for Ba and 98 cm^{-1} for Sr. The bare frequency of Ca is 115 cm^{-1}, which is slightly larger. In any case, it is clear that the full phonon calculation exhibits a lower frequency of filler vibrations than the corresponding bare frequency, which indicates the existence of significant coupling between the filler vibration and the Sb shell nearby.

It is also worth noting that the Ca-dominated lowest optical mode frequency is lower than that of the Ba mode, despite the atomic mass difference. A similar observation was made for $(Ca,Sr,Ba)Fe_4Sb_{12}$ in Ref. 43, where the Einstein temperatures of these compounds were compared. Therefore, the interatomic force constants between the filler and nearby atoms vary significantly from one compound to another. We

TABLE III. Frequencies and characters of two lowest optical modes at Γ. For unfilled $CoSb_3$, values from a previous study (Ref. 41) are also provided for comparison.

	Sb ring motion	$BaCo_4Sb_{12}$ (cm^{-1})	$SrCo_4Sb_{12}$ (cm^{-1})	$CaCo_4Sb_{12}$ (cm^{-1})	$CoSb_3$ (cm^{-1})	$CoSb_3$ (Ref. 41) (cm^{-1})
Lowest	Translation (F_u)	71	63	55	80	78
Second lowest	In-plane rotation (F_g)	90	88	84	83	84

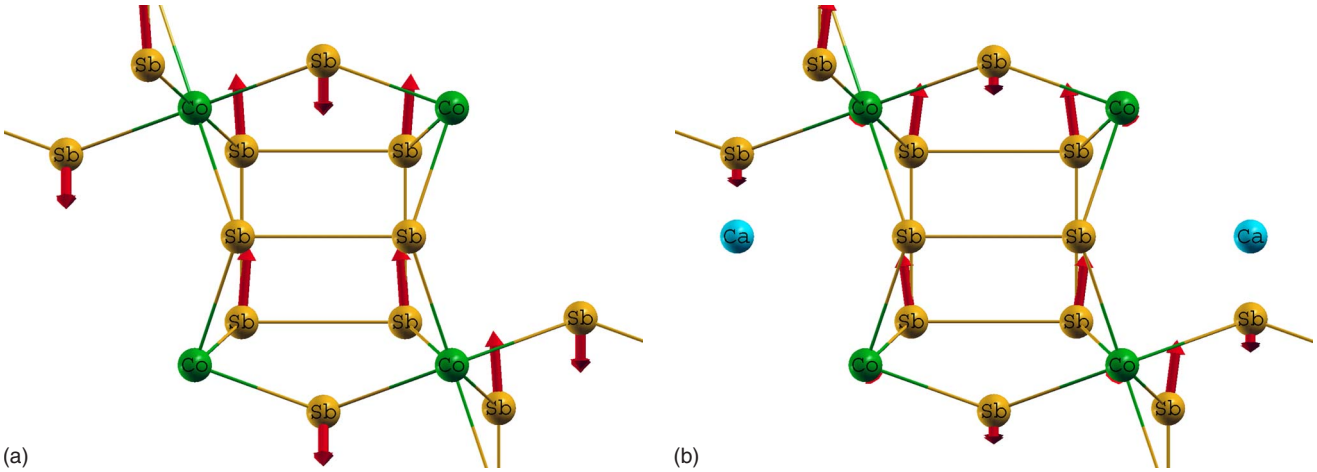

FIG. 12. (Color online) Typical mode shapes observed in the first lowest optical modes at Γ, focused at an Sb ring: (a) $CoSb_3$ and (b) $CaCo_4Sb_{12}$. Visualized with XCRYSDEN (Ref. 42). The motions of Ca atoms are not shown for clarity.

quantify this effect by comparing the largest singular values[44] of the interatomic force-constant matrices $C_{I,\alpha;J,\beta} = \frac{\partial^2 E}{\partial \mathbf{R}_{I,\alpha} \partial \mathbf{R}_{J,\beta}}$. Here, I and J are the indices of nearest atoms, and α and β indicate Cartesian components. The results are presented for strongly interacting pairs in Table IV. Due to the global change in the lattice parameter, interactions between nearest atoms should become weaker, as we proceed from unfilled $CoSb_3$ to filled compounds and also from $CaCo_4Sb_{12}$ to $BaCo_4Sb_{12}$. Though this general trend is recognized in our results, exceptions do occur due to local distortions around fillers. The interaction between the filler and the nearby Sb atoms becomes significantly stronger as we switch from $CaCo_4Sb_{12}$ to $BaCo_4Sb_{12}$. The force constants between the longitudinal pair of Sb atoms increase as well, due to the filler-induced distortion of Sb rings, which has been discussed in Sec. III A. The filler atom pushes its neighboring Sb atoms, making the longitudinal Sb pairs shorter and the transverse Sb pairs longer. The larger the filler is, the more severe the distortion becomes. As the result, the force constants between the longitudinal pair increases as the ionic radius of the filler increases. The frequency trend we observe in the lowest optical modes in filled skutterudites is, hence, derived from the interatomic force constants of the filler-Sb pair and those of the longitudinal Sb pair, which compensate the difference in filler masses. The result indicates that both the mass of the filler and the interatomic force constants are important in determining the frequency of the filler-dominated modes in skutterudites. In particular, it suggests that the local vibration of fillers does not depend only on the filler sizes and masses but also on the force constants of Sb-Sb pairs. This observation may be of importance in designing new compositions with lower thermal conductivity.

A cautionary comment is given at this point: the symmetry character of the lowest optical modes we observe does not exactly match that of $LaFe_4Sb_{12}$ obtained from a force-constant model, where an A_u mode was predicted as the second lowest optical mode at Γ.[16] The details of phonon characters, hence, may be dependent on the choice of the filler element.

IV. SUMMARY

Our calculations demonstrate that alkaline-earth or alkali-metal filling has various structural, electronic, and vibra-

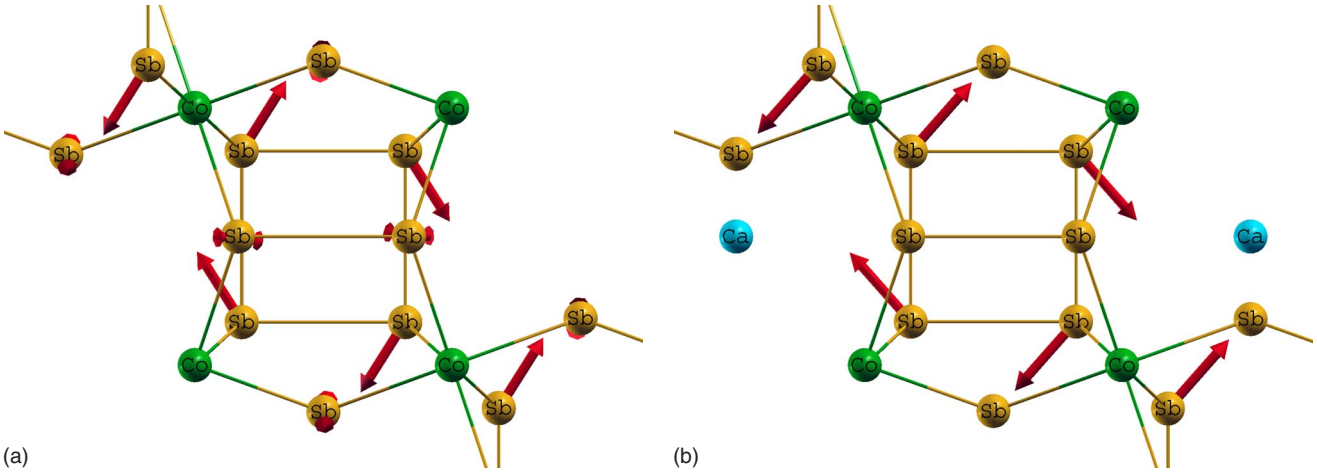

FIG. 13. (Color online) Typical mode shapes observed in the second lowest optical modes at Γ, focused at an Sb ring: (a) $CoSb_3$ and (b) $CaCo_4Sb_{12}$. Visualized with XCRYSDEN (Ref. 42).

TABLE IV. Largest singular value of the interatomic force-constant matrix between each pair of nearest atoms ($Ry/bohr^2$). The direction of each Sb pair respect to two nearby filler sites is also denoted in parenthesis (L: longitudinal and T: transverse).

	Filler-Sb	Sb-Sb (L)	Sb-Sb (T)	Co-Sb
$BaCo_4Sb_{12}$	0.0359	0.0716	0.0631	0.0713
$SrCo_4Sb_{12}$	0.0281	0.0611	0.0698	0.0776
$CaCo_4Sb_{12}$	0.0219	0.0529	0.0760	0.0826
$CoSb_3$	N/A	0.0583	0.1012	0.0927

tional effects in $CoSb_3$ skutterudite systems. Besides the global structural impact on the lattice parameter, a filler introduces locally confined changes in the atomic structure around itself. Soft Sb rings, which are repelled away from the filler, accommodate the local distortion and prevent its long-range propagation.

Electronic band structure, including the band gap at Γ, is sensitive to global and local atomic structures. As typically observed in covalent systems, the direct band gap decreases when the volume increases, which can result either from an external stress or from introduction of fillers with large ionic radii. On the other hand, it is found that the extra electrons donated from a filler to the $CoSb_3$ host structure have the tendency of increasing the band gap, thus competing against the effect of volume increase in filled compounds.

Linear-response calculations have been performed in order to investigate phonon dispersions in filled compounds. In $(Ca,Sr,Ba)Co_4Sb_{12}$, filler-dominated vibration modes appear as the lowest optical modes at Γ, which are mostly localized, that is, decoupled from the other vibrations. Strong similarity of these lowest optical modes in filled compounds to the Sb dominated, lowest optical modes in unfilled $CoSb_3$ is observed, which suggests that the filler-dominated vibration modes originate from the corresponding modes in the unfilled system. Consequently, the motion of the filler is strongly coupled with nearby Sb atoms, resulting in significant discrepancy between the bare frequency and the actual phonon mode frequency of filler vibrations. Additionally, it is found that not only the mass of the filler but also the interatomic force constants determining the filler-dominated vibration frequencies. Overall, it is shown that the fillers' vibrations exhibit nontrivial aspects in skutterudites even at the harmonic level.

ACKNOWLEDGMENTS

The study was carried out as part of the MIT Energy Initiative Program, of which Robert Bosch LLC is a member since 2008. The authors wish to thank S. Park at Robert Bosch Thermotechniek BV (Netherlands), A. Kojic at Robert Bosch LLC (U.S.), T. Eckl, F. Felten, and A. Martinez-Limia at Robert Bosch GmbH (Germany), D. Volja, Q. Hao, and G. Chen at Massachusetts Institute of Technology, Z. Ren at Boston College, and S. LeBlanc, Y. Gao, and K. Goodson at Stanford University for providing supports.

[1] B. Poudel, Q. Hao, Y. Ma, Y. Lan, A. Minnich, B. Yu, X. Yan, D. Wang, A. Muto, D. Vashaee, X. Chen, J. Liu, M. S. Dresselhaus, G. Chen, and Z. Ren, Science **320**, 634 (2008).
[2] K. Momma and F. Izumi, J. Appl. Crystallogr. **41**, 653 (2008).
[3] D. T. Morelli, T. Caillat, J. P. Fleurial, A. Borshchevsky, J. Vandersande, B. Chen, and C. Uher, Phys. Rev. B **51**, 9622 (1995).
[4] T. Caillat, A. Borshchevsky, and J. P. Fleurial, J. Appl. Phys. **80**, 4442 (1996).
[5] G. S. Nolas, D. T. Morelli, and T. M. Tritt, Annu. Rev. Mater. Sci. **29**, 89 (1999).
[6] M. M. Koza, M. R. Johnson, R. Viennois, H. Mutka, L. Girard, and D. Ravot, Nature Mater. **7**, 805 (2008).
[7] J. L. Feldman, D. J. Singh, I. I. Mazin, D. Mandrus, and B. C. Sales, Phys. Rev. B **61**, R9209 (2000).
[8] P. Ghosez and M. Veithen, J. Phys.: Condens. Matter **19**, 096002 (2007).
[9] J. Yang, W. Zhang, S. Q. Bai, Z. Mei, and L. D. Chen, Appl. Phys. Lett. **90**, 192111 (2007).
[10] C. Uher, Semicond. Semimetals **68**, 139 (2001).
[11] D. J. Singh, Semicond. Semimetals **70**, 125 (2001).
[12] D. J. Singh and W. E. Pickett, Phys. Rev. B **50**, 11235 (1994).
[13] J. O. Sofo and G. D. Mahan, Phys. Rev. B **58**, 15620 (1998).
[14] I. Lefebvre-Devos, M. Lassalle, X. Wallart, J. Olivier-Fourcade, L. R. Monconduit, and J. C. Jumas, Phys. Rev. B **63**, 125110 (2001).
[15] H. Sugawara, Y. Abe, Y. Aoki, H. Sato, M. Hedo, R. Settai, Y. Onuki, and H. Harima, J. Phys. Soc. Jpn. **69**, 2938 (2000).
[16] J. L. Feldman, D. J. Singh, C. Kendziora, D. Mandrus, and B. C. Sales, Phys. Rev. B **68**, 094301 (2003).
[17] X. Shi, W. Zhang, L. D. Chen, and J. Yang, Phys. Rev. Lett. **95**, 185503 (2005).
[18] K. Akai, H. Kurisu, T. Moriyama, S. Yamamoto, and M. Matsura, *Proceedings of the 17th International Conference on Thermoelectrics* (IEEE, New York, 1998), pp. 105–108.
[19] K. Akai, H. Kurisu, T. Shimura, and M. Matsura, *Proceedings of the 16th International Conference on Thermoelectrics* (IEEE, New York, 1997), pp. 334–337.
[20] P. Hohenberg and W. Kohn, Phys. Rev. **136**, B864 (1964).
[21] W. Kohn and L. J. Sham, Phys. Rev. **140**, A1133 (1965).
[22] S. Baroni, S. de Gironcoli, A. Dal Corso, and P. Giannozzi, Rev. Mod. Phys. **73**, 515 (2001).
[23] P. Giannozzi, S. Baroni, N. Bonini, M. Calandra, R. Car, C. Cavazzoni, D. Ceresoli, G. L. Chiarotti, M. Cococcioni, I. Dabo, A. Dalcorso, S. Fabris, G. Fratesi, S. Degironcoli, R. Gebauer, U. Gerstmann, C. Gougoussis, A. Kokalj, M. Lazzeri, L. Martinsamos, N. Marzari, F. Mauri, R. Mazzarello, S. Paolini, A. Pasquarello, L. Paulatto, C. Sbraccia, S. Scandolo, G. Sclauzero, A. Seitsonen, A. Smogunov, P. Umari, and R. Wentzcovitch, J. Phys.: Condens. Matter **21**, 395502 (2009).
[24] J. P. Perdew and A. Zunger, Phys. Rev. B **23**, 5048 (1981).
[25] G. Madsen and D. Singh, Comput. Phys. Commun. **175**, 67

(2006).
[26] P. Carrier, R. Wentzcovitch, and J. Tsuchiya, Phys. Rev. B **76**, 064116 (2007).
[27] R. Wentzcovitch, VLAB Themordynamics Package (2006), http://www.vlab.msi.umn.edu/
[28] L. Kleinman and D. M. Bylander, Phys. Rev. Lett. **48**, 1425 (1982).
[29] D. R. Hamann, M. Schlüter, and C. Chiang, Phys. Rev. Lett. **43**, 1494 (1979).
[30] D. Vanderbilt, Phys. Rev. B **41**, 7892 (1990).
[31] D. G. Luenberger, *Linear and Nonlinear Programming*, 2nd ed. (Kluwer Academic, Norwell, MA, 2003).
[32] H. Takizawa, K. Miura, M. Ito, T. Suzuki, and T. Endo, J. Alloys Compd. **282**, 79 (1999).
[33] R. D. Shannon, Acta Crystallogr., Sect. A: Cryst. Phys., Diffr., Theor. Gen. Crystallogr. **32**, 751 (1976).
[34] T. Schmidt, G. Kliche, and H. D. Lutz, Acta Crystallogr., Sect. C: Cryst. Struct. Commun. **43**, 1678 (1987).
[35] H. Rakoto, E. Arushanov, M. Respaud, K. M. Broto, J. Leotin, Ch. Kloc, E. Bucher, and S. Askenazy, Physica B **246-247**, 528 (1998).
[36] H. Rakoto, M. Respaud, J. M. Broto, E. Arushanov, and T. Caillat, Physica B **269**, 13 (1999).
[37] D. Mandrus, A. Migliori, T. W. Darling, M. F. Hundley, E. J. Peterson, and J. D. Thompson, Phys. Rev. B **52**, 4926 (1995).
[38] E. Z. Kurmaev, A. Moewes, I. R. Shein, L. D. Finkelstein, A. L. Ivanovskii, and H. Anno, J. Phys.: Condens. Matter **16**, 979 (2004).
[39] D. W. Jung, M. H. Whangbo, and S. Alvarez, Inorg. Chem. **29**, 2252 (1990).
[40] J. L. Feldman and D. J. Singh, Phys. Rev. B **53**, 6273 (1996).
[41] D. J. Singh, L. Nordstrom, W. E. Picket, and J. L. Feldman, *Proceedings of the 15th International Conference on Thermoelectrics* (IEEE, New York, 1996), pp. 84–86.
[42] A. Kokalj, Comput. Mater. Sci. **28**, 155 (2003).
[43] W. Schnelle, A. Leithe-Jasper, H. Rosner, R. Cardoso-Gil, R. Gumeniuk, D. Trots, J. A. Mydosh, and Y. Grin, Phys. Rev. B **77**, 094421 (2008).
[44] G. Strang, *Linear Algebra and Its Applications*, 4th ed. (Brooks-Cole, Belmont, MA, 2005).